Aalborg Universitet

A USRP-Based Multi-Antenna Testbed for Reception of Multi-Site Cellular Signals

Izydorczyk, Tomasz Stanislaw; Tavares, Fernando Menezes Leitão; Berardinelli, Gilberto; E. Mogensen, Preben

Link to publication from Aalborg University

A USRP-Based Multi-Antenna Testbed for Reception of Multi-Site Cellular Signals

TOMASZ IZYDORCZYK [ID][1], **FERNANDO M. L. TAVARES** [ID][1],
GILBERTO BERARDINELLI [ID][1], **AND PREBEN MOGENSEN** [ID][1,2]

[1]Wireless Communication Networks Section, Department of Electronic Systems, Aalborg University, 9220 Aalborg, Denmark
[2]Nokia Bell Labs, 9220 Aalborg, Denmark

Corresponding author: Tomasz Izydorczyk (ti@es.aau.dk)

ABSTRACT This paper presents a design of a Software Defined Radio (SDR) multi-antenna testbed able to record live cellular signals from multiple sites. This measurement setup based on Universal Software Radio Peripheral (USRP) boards, is used to record live Long Term Evolution (LTE) signals in sub-6 GHz frequency bands. Due to recording of raw I&Q samples, this fully digital testbed is suitable for variety of research activities spanning channel characterization and beamforming performance evaluation. We propose a phase calibration method based on transmission of a single out of band tone to overcome the uncertainty introduced by the USRP's lack of phase alignment. We demonstrate two use cases where the proposed testbed can be used and we validate its performance during two measurement campaigns with self-generated and real cellular signals.

INDEX TERMS Antennas and propagation, beam steering, measurement techniques, multi-antenna, SDR, USRP.

I. INTRODUCTION

Multiple antenna systems are well known to increase capacity and reliability of the communication links. For many years, theoretical and simulation works have shown the achievable gains when large antenna arrays are used [1]. Such studies rely on the channel models existing in the literature derived from measurement campaigns. Moreover, field trials using wireless platforms and testbeds are conducted to provide algorithm's performance evaluation in real deployment scenarios. New use cases including Industry 4.0 [2], Vehicle-to-Everything (V2X) [3] or Unmanned Aerial Vehicle (UAV) [4] communications open up new scenarios which may not be properly characterized by existing models. Therefore there is even greater need for further experimental channel modeling as well as empirical studies of multi-antenna algorithms in the mentioned scenarios.

Building large testbeds with multiple antennas is not a trivial task. Although typical requirements of a measurement system are operating frequency, bandwidth and the number of antennas, the design is usually influenced by multiple other factors. One of them is the actual use case which determines

The associate editor coordinating the review of this manuscript and approving it for publication was Davide Comite [ID].

what type of transmitted signal should be used. Very often multi-antenna testbeds are complemented with a self-made transmitter (single or multi-antenna) radiating self-generated excitation signal. By using such an approach, different measurements can be conducted in controlled scenarios with exact control of the transmitter (TX) and receiver (RX) positions, the type of radiated signal and the synchronization between nodes [5].

However there are certain situations in which using a self-made transmitter can be impractical and pose unnecessary constraints on the designed experiment. Studies on algorithms as beamforming or Interference Rejection Combining (IRC) receivers require gathering samples in the presence of interference. In these situations, multiple transmitting nodes imitating WiFi access points or cellular base stations are required to be deployed relatively far from each other in order to emulate the target and interfering signals. Very often they would need to be placed in hardly accessible places like roofs of the buildings or lamp posts. Although such a measurement system using self-made transmitters can be deployed, scalability may become cumbersome. To obtain reliable results, numerous deployment scenarios need to be tested, requiring time consuming redeployments of the transmitting nodes.

Similar problems may occur if the studied use-case demands measuring over a large geographical area. V2X or UAV communications are some exemplary studies that require gathering numerous samples in different scenarios. Several redeployments of the self-made transmitter might be required to efficiently cover large areas; this might render the measurement campaign unfeasible.

One of the potential alternative is to measure signals directly from live cellular networks. In this case, the redeployment time is shortened as only the receiver needs to be repositioned. Moreover, obtained results are more reliable since they are taken from a real network deployment. Another benefit of using live cellular networks is the possibility of concurrent recording of signals incoming from multiple visible cells. As each of the cell has its own identifier - Cell ID, multiple cells can potentially be decoded from the same data snapshot, leading to expansion of the recorded data set. Multiple visible cells recorded during the same data snapshot can also be seen as interference with respect to a target cellular signal. The ability to differentiate among them can be beneficiary when studying the performance of interference rejection or receive beamforming algorithms.

Although as shown in Section II, many multi-antenna testbeds are reported in the literature, none of them operates using live cellular signals as for example Long Term Evolution (LTE). The measurements of live cellular signals impose several constraints on a measurement system. Due to lack of control of the transmitter, the TX-RX synchronization would only be achieved if real-time signal decoding is performed. Moreover the increased receiver complexity with respect to a self-generated excitation signal can discourage its possible usage. However many research activities do not require any real time processing and their target research objectives can be achieved offline, by recording raw I&Q data samples and processing them later using software. Works in [6] and [7] are some example use cases where offline processing is used.

This work describes a novel measurement methodology, in which a large multi-antenna testbed is used to record live cellular signals transmitted from multiple base stations. The testbed was built for a wide range of studies related to V2X and UAV communications including spatial channel characterization and beamforming performance evaluation. The major focus is placed on the flexibility of the measurement system as this fully digital design is based on Universal Software Radio Peripheral (USRP) boards and can operate with any cellular signals. The proposed methodology and hardware design are complemented by the practical description of the offline post-processing methods covering LTE signal reception using Matlab's LTE toolbox [8] and channel characterization using Space Alternating Generalized Expectation-Maximization (SAGE) algorithm [9]. Up to the best of the authors knowledge, this is the first testbed with a large antenna array capable of working with live cellular systems presented in the literature.

The rest of this article is structured as follows. An extensive literature survey on the existing testbeds is presented in Section II. Section III discusses the general system design requirements. It is followed by Section IV focusing on the system implementation in both hardware and software. As a part of the hardware description, in Section IV-B the problem of establishing phase synchronization between boards is described. Later in Section V two examples of postprocessing methodology are presented. Section VI presents the validation of the overall concept in real environments. Finally, Section VII discusses the potential use cases in which the proposed testbed is a suitable choice. The work is concluded in Section VIII.

II. LITERATURE SURVEY

Many research activities use large multi-antenna testbeds. Unfortunately, very frequently these articles are focused only on the results obtained using them, leaving only a small part of an article for the actual testbed description. However the testbed design in both hardware and signal processing steps is a non-trivial task. Usually measurement setups can be divided in three distinct categories: switched antenna testbeds, fully digital custom-built testbeds (based on Application-Specific Integrated Circuits (ASICs), Digital Signal Processors (DSPs) or Field-Programmable Gate Arrays (FPGAs)) and one's built based on Software Defined Radios (SDRs). All types of a measurement system have their distinctive features. If a real time, high throughput capability is necessary, a dedicated ASIC-based testbed with algorithms being developed on FPGA chips is the most common design choice. If fast prototyping and high reconfigurability are desired, SDR-based testbeds are the best option.

In the remaining of this section, a literature survey presenting multi-antenna testbeds is presented. Please note that the proposed literature list is by any means not exhaustive, but is rather a subjective list of works where, in the authors opinion, the used testbeds were sufficiently described.

The literature on channel sounders built based on the switching antenna systems is broad. The descriptions of multiple developed channel sounders can be found in the deliverables of some large international projects like WINNER [5] or TSUNAMI [10]. Also many smaller research activities use the switched antenna systems. In [3], the 16-elements switched antenna system was used to study the vehicle-to-vehicle (V2V) cluster-based propagation channel. Similar work is presented in [11] where a real-time channel sounder for V2V propagation studies at 5.9 GHz is presented with the focus on spatial channel characterization. This article together with [12] are examples of testbeds where a switched array is used in conjunction with a single USRP board providing the Radio Frequency (RF) chain.

A comprehensive survey on different types of a fully digital custom-built testbeds with large antenna arrays is presented in [13]. This work contains three example of testbeds built based on ASIC, FPGA and DSP components. Their potential use cases are also discussed. Work in [14] presents a custom built testbed with a large 12-elements circular array used to study the potential mismatches in the beamforming directions

between Downlink (DL) and Uplink (UL). Another large testbed using dedicated hardware is presented in [15]. It is a 16x16 multi-user MIMO system operating using indoor Wi-Fi to study the effects of the increased number of users on a transmission bit rate. Interesting work on interference alignment techniques using a multi-user MIMO testbed is presented in [16]. In this work, authors use a customized testbed working in a 5 GHz band to measure and exploit the interference channels caused by multiple users. Finally, authors in [7] focus on receive beamforming using a testbed with a 4-element antenna array in the 2 GHz frequency band and [17] focuses on beamforming with side lobe level reduction where beams are created using a testbed built with a dedicated hardware and 8-element array.

There are many multi-antenna testbeds built based on SDRs reported in the literature confirming the ongoing trends. Authors in [18] use a self-built SDR setup to study the impact of imperfections in hardware and channel estimation inaccuracies using a 4x4 multi-user multi-antenna setup. A four antennas system to study the DoA estimation and digital beamforming for jamming signal avoidance in satellite communication is described in [19]. The authors use a single dual-port USRP equipped with an additional daughter-board installed as RF-port extension. By using such, they are able to accommodate all four antennas within a single USRP omitting the burden of providing phase calibration between different boards as it would be required if two dual-port USRPs are used.

Multi-antenna testbeds built by connecting multiple USRP boards in sub-6 GHz bands are also available in the literature. The researchers from Lund university developed a 100-antennas testbed for real time massive MIMO evaluation [20] and together with Bristol University even larger 128-antennas setup presented in [21]. However their usage was still constrained to receive self-generated cellular signal and was not extended to operate with live signals. Works in [22] and [23] focus on adaptive beamformers using a 4 and 3 elements antenna arrays respectively, where each antenna is connected to a different USRP board. In [24] and [25] the antenna arrays (up to 8 antennas in the latter case!) are used for DoA estimation. Finally a USRP-system containing 4 synchronized nodes is used for the localization purposes in [26].

Although as presented in this section, there are many multi-antenna testbeds available in the literature, none of the acknowledged works use them for reception of live cellular signals. Therefore, this article presents a setup extendable to operate with arbitrary number of antennas; thoroughly explaining the process of recording, decoding and utilizing the multi-site transmitted cellular signals for various research purposes.

III. SYSTEM DESIGN
A. SYSTEM REQUIREMENTS
While designing the proposed measurement testbed, multiple different factors were considered. Although the first research

directions to be targeted using the designed testbed were already defined at the design phase (channel characterization for the cellular V2X communication), it was assumed that in the future the proposed testbed will be used for some activities which at this stage had not yet been defined. The ideal envisioned setup should therefore provide flexibility of usage for various research activities including spatial channel characterization or beamforming evaluation, possibly in different frequency bands up to 6 GHz.

To satisfy the envisioned use cases, the designed testbed is required to concurrently measure signals from multiple transmitters using multiple antennas. For the reasons explained in the introduction, it was decided to measure live LTE signals. This requirement impose the use of fully digital system where each antenna port has its own RF chain. The use of switching antenna system, although theoretically possible, would be cumbersome to implement due to channel non-stationarity and challenging transmitter-receiver synchronization. As some research activities may impose special demands on an antenna array, including different number of antennas or a specific antenna configuration, the designed testbed should be adaptable and allow to accommodate different number of antennas with only little changes to the overall hardware architecture.

B. GENERAL DESIGN
To address flexibility demands, it was determined that the designed platform should be based on SDRs and be capable of recording and storing data snapshots containing raw I&Q samples with no real-time processing. By using SDR boards, one can benefit from their high reconfigurability, usual high range of operating frequencies and recorded signal bandwidths. By recording raw, unprocessed data samples, there is no risk that the real-time processing would reduce or prevent certain future activities in post-processing. As some of the potential use-cases may require precise location information, the Global Positioning System (GPS) antenna need to complement the design.

In the described testbed we decided to use the NI USRP 2953R boards as a SDR platform. The operating frequency range from 1.2 GHz to 6 GHz is deemed to be sufficient to assure the flexibility demands. Each board contains two RF chains, therefore multiple boards are required to build a large multi-antenna testbed. The boards can record up to 40 MHz real time bandwidth, which is sufficient to record live LTE signal (with maximum 20 MHz bandwidth). By using additional National Instruments (NI) equipment, further described in the next Section, the remaining design requirements can be fulfilled. A PXI chassis and its embedded controller allow to control multiple boards, while a timing module is used to distribute a common synchronization signal via Octoclocks enabling coherent measurements across all boards. In extreme situations, when desired array size (and therefore number of USRP boards) is larger than the amount of slots available within a PXI chassis, these can be combined to create a multi-chassis acquisition system.

TABLE 1. Reference configuration of a proposed multi-antenna testbed.

| Parameter	General Design	Proposed Implementation
Type of recording platform	Any USRP-type boards	USRP 2953R
Type of recorded signal	Any signal with power above the receiver's sensitivity	live LTE incoming concurrently from multiple base stations
Number of USRP boards	Flexible (For large number of boards, the multi-PXI system would be required)	8 RX and 1 TX board
Number of antennas	Flexible (Depends on the amount of the USRP boards)	16 RX and 1 TX
Array configuration	Flexible (although the calibration procedure might need to be adjusted)	UCA
Carrier frequencies	1.2 - 6 GHz	1.845 GHz
Signal bandwidth	Depends on a use case (up to 40 MHz)	40 MHz
Sampling rate	Up to 200 MS/s	40 MS/s
Length of the recorded signal	Flexible (depends on a sampling rate and signal bandwidth)	100 ms
Frequency accuracy	Up to 5 ppb with GPS-locked OCXO signal	25 ppb
Phase accuracy	Depends on an implemented calibration procedure	$\leq 1^o$
Receiver sensitivity	Depends on signal bandwidth and minimum SINR	~ -114 dBm assuming 1.08 GHz bandwidth of MIB, minimum SINR of -5 dB and USRP receiver window reference level set to -25 dB

Although, the proposed system architecture matches the design requirements, for some use cases it is not sufficient. Beamforming applications or DoA estimation algorithms require, a tight phase synchronization over all antennas in order to exploit small phase differences in their signal processing algorithms. The multi-USRP platform designed as proposed would not support these applications as it is known that the USRP boards are not phase-coherent [24]. Therefore an extra phase calibration procedure needs to be implemented. Its details are described later in Section IV-B.

IV. SYSTEM IMPLEMENTATION

A. MEASUREMENT SYSTEM

The presented measurement system is composed of a multi-antenna receiver as well as additional hardware used for transmission of the calibration signal needed to phase-align all USRP boards as will be described in Section IV-B. Figure 1 presents the block diagram of the setup with calibration part highlighted by a green dashed line. Besides, Table 1 summarizes the general and implementation-specific configurations of the designed testbed. For the envisioned use cases, 1.845 GHz operating carrier frequency was chosen. This particular carrier frequency is the middle of LTE band 3 occupied by two Danish telecom operators with more than 50 base stations deployed per operator. Such choice allows to double the potential measurements using the same testbed and antenna configuration.

The receiver features a 16-antennas Uniform Circular Array (UCA), which has been manufactured on an aluminum ground plane. The reason for using UCA rather than a linear array, is its ability to scan the incoming signals in all 360° without ambiguity. The number of antennas was selected as a good trade-off between setup complexity and achievable system resolution. Antennas are connected to 8 USRP 2953R boards, each providing two separate RF chains. All boards are connected to an embedded controller using Peripheral
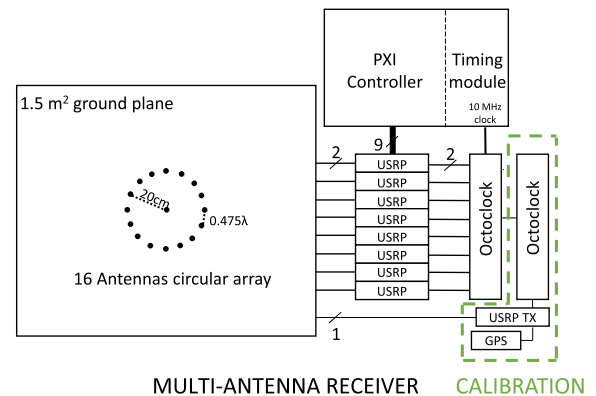


FIGURE 1. Measurement system schematic.

Component Interconnect (PCI) bus. The synchronization signal is generated by an Oven Controlled Crystal Oscillator (OCXO) and distributed to all USRPs using an Octoclock.

The receiving part is complemented with an additional ninth USRP board (and antenna located in the center of the array), used for generation of the calibration signal. The board is connected to the same embedded controller and synchronized to the same synchronization signal using a second Octoclock. In the remaining of this Section, each hardware element is described.

1) UNIFORM CIRCULAR ARRAY DESIGN

The UCA is composed of 16 monopoles placed on an 1.5 m × 1.5 m aluminum ground plane. The ground plane has been manufactured with bent edges to reduce border effects arising due to its finite length and therefore limit the potential up-tilt of the antenna radiation pattern. The array has been designed to work in the downlink part of LTE Band 3 (center frequency of 1.845 GHz), which corresponds to a circular radius of 20 cm, wavelength $\lambda = 0.1625$ m and antenna spacing 0.475λ. Proposed design was simulated
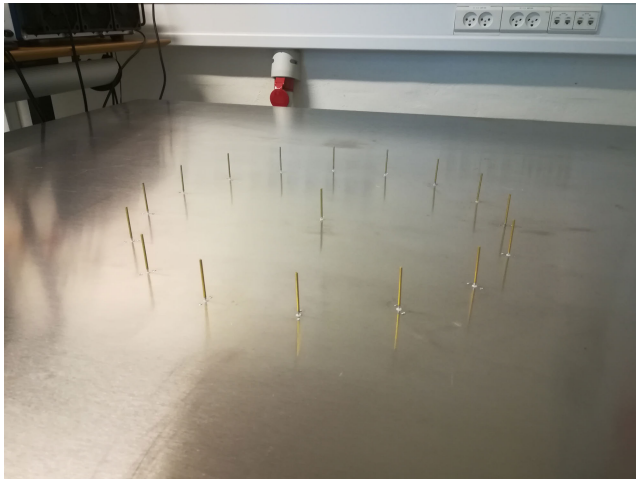
FIGURE 2. Antenna array used in the setup.

FIGURE 3. Assembled setup.

in CST Studio - a software among others used for antenna design and simulation. Results showed that array's far-field radiation pattern can be very well approximated by an omnidirectional pattern in the azimuth domain. Antenna array is meant to be installed on the roof of a vehicle, to facilitate drive tests. To minimize the risks of possible short circuit between antennas and ground plane in case of rain and to prevent any physical damage, a Styrofoam radome of 25 cm radius covers the monopoles on the ground plane. Figure 2 presents the complete antenna array design before the radome installation.

2) NI USRP 2953R

Eight USRP boards have been used as RF chains. Each board is equipped with two separate RF chains, which are configurable using NI LabView Communications software. An additional ninth USRP was used as a transmitter for the calibration signal. As already mentioned, this model of the USRP operates in the frequency range from 1.2 GHz to 6 GHz, with up to 40 MHz real time bandwidth, which is sufficient to record live LTE signal (that can occupy up to 20 MHz bandwidth).

The USRP boards perform digital down conversion and stream the I&Q samples via fast PCI bus to the controller. The described setup is able to record the ''raw'' radio signals. The processing of the LTE signal, including frame alignment, cell search, demodulation of the reference signals etc. is done offline using for example Matlab LTE toolbox.

3) NI PXIE-1085 AND NI PXIE-8135

NI PXIe-8135 is a powerful embedded controller for PXI Express systems, which can be used to control the measurement setup using LabView Communications software as described later in Section IV-C. The controller is installed within the PXIe-1085 chassis, which in addition contains sixteen hybrid slots with up to 24 GB/s connection speed and 1 PXIe timing slot. Nine slots are used as extension boards to connect all USRPs and Timing module (OCXO board) is used in the timing slot. By using the chassis, there is a possibility
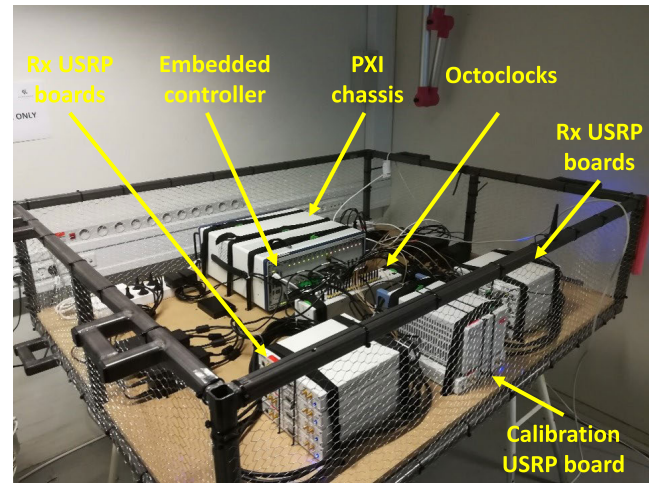
to use even more antenna elements as remaining empty slots can be used to accommodate more receiving USRP boards and extend the system to larger antenna arrays.

4) OCTOCLOCKS CDA-2990 AND NI PXIE-6674T

Even though each USRP board is equipped with its own local oscillator, coherent data detection requires data to be collected with time and frequency synchronized system, while beamforming or DoA estimation algorithms require even tighter phase alignment between all antennas. Frequency synchronization between different boards can be achieved by providing an external 10 MHz reference clock. Also a Pulse Per Second (PPS) trigger, in this case generated by one of the USRP boards, must be distributed to all of the boards, so that its rising edge initializes the reception on all boards.

The NI PXIe-6674T Timing Module provides a 25 parts per billion (ppb) precision 10 MHz clock, which is installed as an extension board within the PXI chassis. The 10 MHz clock is then distributed to two eight ports Ettus Octoclocks CDA-2990 which further distribute it coherently to all nine USRP boards. To avoid any ambiguities in delays and due to limited number of ports per Octoclock, all eight receiving USRP boards are connected to the single Octoclock (as shown on Figure 1), while the USRP used for calibration purpose is connected to the second one.

Figure 3 presents the assembled measurement setup before its connection with the antennas using 3 meter long RG233 cables. It is worth to note that although the proposed measurement system was designed (and is further described) as a multi-antenna receiver, it can potentially be used as a multi-antenna transmitter, although some changes to the overall design methodology would be required. First, the receiver's software as described in Section IV-C would need to be upgraded to incorporate the transmitter. Second, if the phase alignment between all transmitting antennas is required, the proposed calibration would become insufficient and would need to be redesigned to occur in real-time rather than in post-processing.
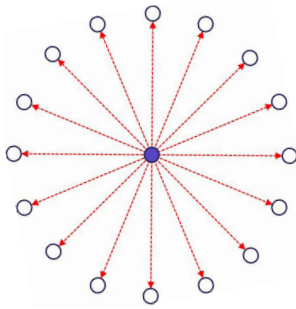
FIGURE 4. Principle of calibration tone transmission.

FIGURE 5. Received signal spectrum.

B. CALIBRATION PROCEDURE

Time and frequency synchronization as explained in previous section is not sufficient if signals recorded by the proposed testbed are to be used for beamforming or DoA estimation where phase differences are important. Even though all USRP boards are phase coherent, they are not phase aligned (each board starts receiving with a different unknown phase offset) and therefore a calibration method is required to compensate this misalignment.

Different methods for calibration are proposed in the literature. All of them are however related to the same principle - generation of the known calibration signal and its redistribution to all USRPs. Authors in [24] and [26] use an additional USRP board to generate the signal. By using a RF power divider, the signal is distributed using antenna cables of the same length to all boards. The drawback of this method is the eventual loss of one transceiver chain in each receiving USRP just for calibration.

Over the air calibration is proposed in [22] and [25]. In both works the calibration signal is transmitted wirelessly to the receiving array. In post-processing the signal is filtered and phase-difference between boards is computed assuming that it was only caused by the initial USRP phase difference. As both works use linear array, the systematic phase difference occurring due to unequal signal's travel distance from the reference antenna to each antenna element can be calculated beforehand and corrected.

In this project, a low power Out-of-Band (OoB) calibration signal is transmitted from the additional antenna placed in the center of the array. In this case, given the array symmetry, all antennas will receive the signal with equal delay, power and phase as illustrated on Figure 4. Therefore no additional phase shift between antenna elements is observed as if a linear array would be used.

The calibration signal is a single tone transmitted approximately 5 MHz away from the edge of the target LTE band with -50 dBm transmit power. Such low power prevents significant interference to other systems potentially transmitting in this band. OoB transmission is also beneficial as it does not interfere with the received LTE signal. Before the final decision on frequency used to transmit the calibration tone, frequency spectrum is scanned with a spectrum analyzer in order to avoid the choice of frequencies that are occupied
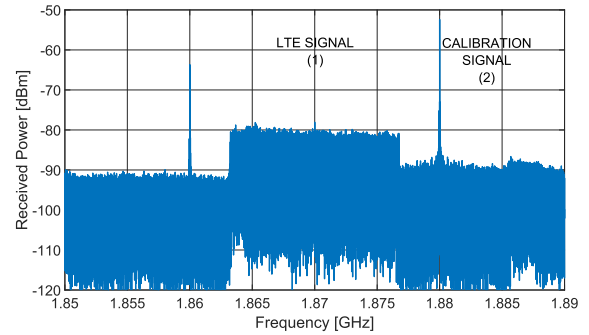
by another system, potentially interfering with the calibration tone. Figure 5 presents a sample recorded signal in 1.8 GHz band with LTE (1) and Calibration signals (2).

After samples are recorded, first step before any array processing is the system calibration. Calibration tone is separated from the received signal by means of digital filtering in frequency domain. Then the frequency position of its actual peak is found based on maximum energy detector for all the receiving antennas. Assuming the received phase of the signal on one of the antennas as a reference, the phase difference can be computed for all remaining ones. Finally, the entire received sequence is phase shifted for the remaining fifteen data streams according to the computed difference. The proposed calibration method effectively reduces the phase offset down to less than 1°, which is sufficient for accurate beamforming and DoA estimation as presented later in Sections VI and VII.

C. MEASUREMENT SOFTWARE DESIGN

Measurements are conducted using LabView Communications software installed on the PXI embedded controller. The setup has been designed in a flexible way, such that the duration of a measurement snapshot can be adjusted up to 350 ms of continuous recording. Limitation of recording time is the result of limited size of Direct Memory Access (DMA) buffer of the USRP board. Besides snapshot duration, the recording periodicity can also be adjusted. Its minimum value is limited by the time required to store all the data on a hard drive. Therefore the designed software offers a flexibility to record short snapshots at higher frequency or longer ones with larger measurement gap between them. This flexibility is especially valuable in case of the drive tests or other use cases in which the receiver changes its position with time.

Designed software is composed of three main threads as presented on Figure 6. First thread is responsible for generation of the calibration signal and its transmission during the receiving time window. When the recorded data is being processed and saved, the transmitter is inactive, to reduce the potential interference caused to the other systems. Second thread is used for periodic acquisition of the GPS information recorded using NI-compatible magnetic mount GPS antenna, connected to one of the USRP boards. Finally, the third thread receives the signal. Later it performs simple data compression
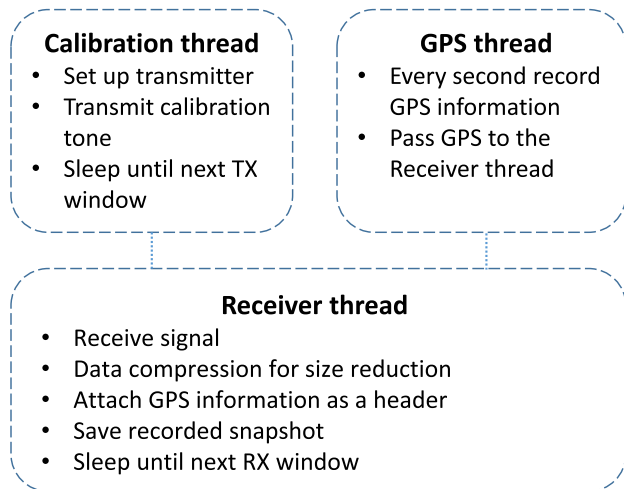
Calibration thread
- Set up transmitter
- Transmit calibration tone
- Sleep until next TX window

GPS thread
- Every second record GPS information
- Pass GPS to the Receiver thread

Receiver thread
- Receive signal
- Data compression for size reduction
- Attach GPS information as a header
- Save recorded snapshot
- Sleep until next RX window

FIGURE 6. Block diagram of the measurement software.

Beamforming flow chart

Phase Calibration
Calibrate the random phase offset of each of the USRP boards as in Section (IV)

Beamforming
Create a beam towards direction θ, according to equation (1)

LTE receiver chain
PSS and SSS synch. → Coarse channel estimation → MIB decode → Frequency offset correction → Full channel estimation (Input for SAGE estimation) → SIB1 decode

Results comparison
Compare the reported SIB1 SINR among different beamformed directions θ

FIGURE 7. Post-processing flowchart for beamforming evaluation.

to reduce the size of the data (which speeds up the saving process), adds header information where GPS information is included and saves each snapshot independently on the hard drive. Finally all three threads wait until the new recording cycle begins according to the desired periodicity.

V. EXAMPLES OF POST-PROCESSING METHODOLOGY

In this Section, two different examples of post-processing are presented, to indicate possible use cases of proposed testbed. First the LTE signal demodulation is presented, followed by channel estimation using SAGE algorithm. The described post-processing is used in the upcoming sections during the validation measurements to showcase the capabilities of the proposed setup. Although data processing is usually use case dependent, the post-processing presented in this section is very generic and can be used as a building block for many diverse, more advanced, research applications.

A. LTE DEMODULATION AND BEAMFORMING

Received signal can be processed to demodulate LTE signals in order to extract common cell information (available in the Master Information Block (MIB) and System Information Block 1 (SIB1)) or to estimate received channel and use it as an input for SAGE processing. The demodulation can be done two-fold. One way is to program the entire LTE receive processing by writing code based on relevant 3GPP standards, as done for example in [27], where the code for correlation-based network synchronization or channel estimation was self-written. An interesting alternative is to use Matlab LTE toolbox. It contains all the relevant functions for signal demodulation. Although this toolbox is primarily used for the simulation-based evaluation of LTE system, as shown in this work, it can also be used for demodulation of the live cellular signals recorded with USRPs.

In the remaining of this section, the potential of using the LTE toolbox is discussed by describing the receive beamforming processing. Although this section is focused
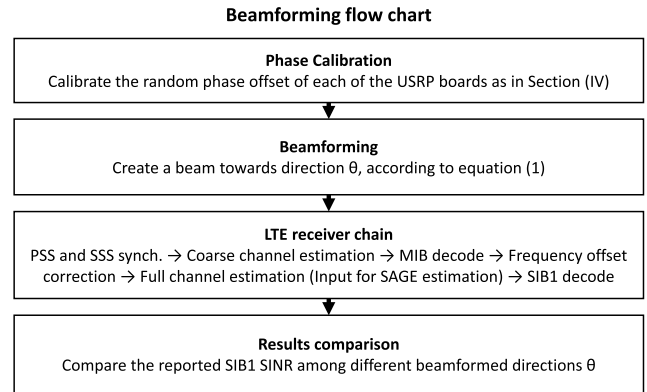
only on the receiving beamforming, other multi-antenna combining techniques including Maximum Ratio Combiner (MRC) or even single antenna processing can be achieved by replacing the beamforming block with the desired antenna processing as described in [28].

Figure 7 presents the flowchart of the data processing. Received signals impinging on the multiple antennas are first phase-calibrated and then beamformed towards the desired angle as below:

$$\mathbf{y} = \left(e^{-2\pi j \frac{r}{\lambda} \cos(\varphi) \cos(\theta - \boldsymbol{\theta})} \right)^H \cdot \mathbf{S} \qquad (1)$$

where $\mathbf{S}$ is the phase-calibrated input data stream, θ and φ refer to the azimuth and elevation angle for a given beam, r is the radius of the antenna array, λ is the wavelength and $\boldsymbol{\theta}$ is the antenna position-dependent column vector of angles of size $[N_{RX} \times 1]$ where N_{RX} denotes number of receiving antennas. $(\cdot)^H$ denotes the hermitian operator.

After beamforming, the resulting data vector $\mathbf{y}$ is obtained and processed by the LTE receiver, where using Matlab's framework, first a LTE synchronization procedure is performed based on LTE synchronization signals (PSS and SSS). In the next steps, there is a frequency and time offset estimation and correction followed by MIB decoding for selected (one or more) Cell-IDs. In this way, all the necessary information required for channel Cell-specific Reference Signal (CRS) extraction are obtained.

After down-sampling to the sampling rate corresponding to the bandwidth of received LTE signal, channel reconstruction based on LTE CRSs can be performed. Moreover, if the entire process is repeated for different Cell-IDs, potential number of transmitting LTE base stations can be deduced. Finally, provided sufficient signal quality, SIB1 can be decoded. If successful, the Error Vector Magnitude (EVM) and Signal to Interference plus Noise Ratio (SINR) of this control channel are computed.

B. CHANNEL PARAMETERS ESTIMATION USING SAGE

SAGE algorithm is a well known, powerful tool to estimate the number of signal taps, their gains, delays, DoAs and doppler shifts. Readers are referred to [9] for details on the algorithm.

Only few examples in the literature can be found where SAGE was used to estimate parameters of the live LTE signal. Even fewer works can be found presenting the insights of its usage such as algorithm's initialization. One example of such work is [27] where authors used continuous chunks of 50 ms of recorded LTE signal (only the CRS grid) for SAGE estimation. At first, they pre-initialize their algorithm to pre-estimate 30 multipath components. After some SAGE iterations, the potential number of multipath components is estimated and the results are refined by running additional 15 iterations of SAGE only for the predicted number of paths.

In this work, similar to [27], the CRS signals are used for SAGE estimation. The main reason for choosing CRS over any other common signals available in LTE is the fact that CRS are equally spread over the entire frequency band and they are always transmitted using the same deterministic pattern, which can be learned from the MIB. Usage of the entire recorded LTE signal would not be feasible as it contains unknown user-specific data transmissions. The transmitted CRS pattern, used in SAGE as a blueprint for channel estimation, is again re-created at the receiver using Matlab LTE toolbox based on information from the MIB.

Contrary to the cited work, our SAGE implementation can work with a flexible length of CRS sequence from 30 ms up to 300 ms. Such range is a consequence of the flexible recording duration as explained in Section IV-C. Algorithm is initialized to estimate 50 paths. However after initial five iterations, all the taps with a path gain minimum 40 dB lower than a maximum path gain are discarded as they are deemed to represent noise. Later another ten iterations of SAGE are run for the remaining, limited number of taps. In the upcoming section, the presented approach and algorithm's implementation are validated using both self-generated and live LTE signals.

VI. SYSTEM VERIFICATION
First step after the design of a measurement testbed is its verification in a known environment. This Section describes two measurement campaigns used for testbed's validation. In the first one, the proper recording, calibration and implementation of a post-processing software (beamforming algorithm and SAGE processing) are validated. By using self-generated LTE signal in a Line of Sight (LoS) scenario, the expected DoA can be inferred from the position of the receiving array and confronted with the estimated one. Second validation campaign is used to test if the proposed testbed can correctly operate with a live LTE signal with presence of interference.

A. MEASUREMENTS USING SELF-GENERATED LTE SIGNAL
In the first measurement, the proposed testbed, its calibration and post-processing methodology were tested in controlled scenario. The target of this measurement was to estimate DoA of the transmitted self-generated LTE signal by using two different methodologies - beam sweeping and SAGE estimation. By using an additional USRP board, the self-generated LTE signal was transmitted with 0 dBm transmit power as shown on Figure 8. The multi-antenna testbed was
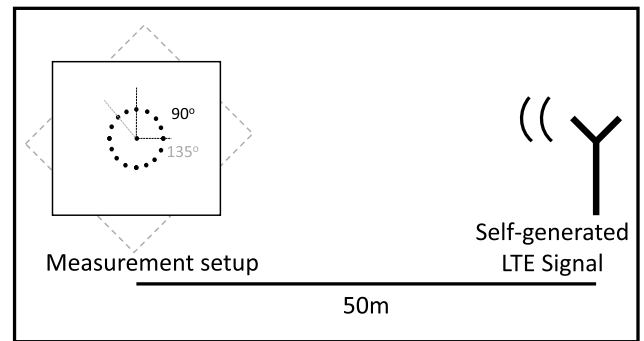

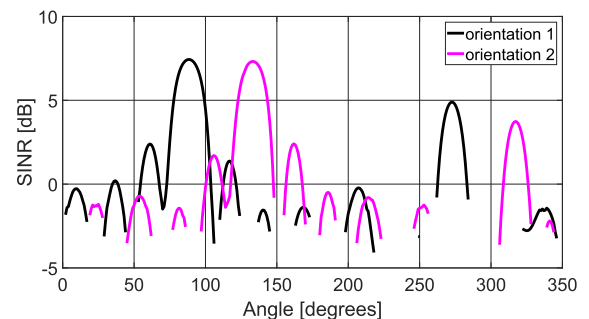**FIGURE 8.** Concept of the first validation campaign.

FIGURE 9. Angular distribution of SINR for self-generated signal.

placed approximately 50 m away in a clear LoS condition with respect to the transmitter. Two 100 ms snapshots of the LTE signal were recorded and the antenna array was carefully positioned in two orientations, such that approximately 90° DoA in orientation 1 and 135° DoA in orientation 2 are expected. If estimation is correct, all building blocks (hardware and software) of the proposed testbed will be validated.

First way of DoA estimation is beam sweeping. It uses the beamforming methodology explained in Section V-A. Recorded signals for both orientations are in the post-processing beamformed towards 360 different directions in the azimuth domain with a step of 1°. 0° elevation angle is assumed. For each beamformed angle, the whole LTE demodulation processing is made and provided successful decoding, SINR of SIB1 is computed.

Figure 9 presents the computed SINR distribution for different beamformed angles. As expected, the maximum SINR values are obtained for the angles close to 90° and 135° respectively, corresponding to the situations when beam was pointed in the direction of the transmitter. The missing SINR values for some angles are related to the angles where SIB1 was not decodable due to insufficient SINR.

The same recorded snapshot was also used to estimate DoA based on SAGE as explained in Section V-B. The estimated channel matrix using LTE toolbox was used as an input for SAGE estimator set to estimate 50 paths. Figure 10 presents the azimuth DoA versus gain for each estimated path. As expected, paths with the highest gain have their corresponding DoA located at approximately 90° for
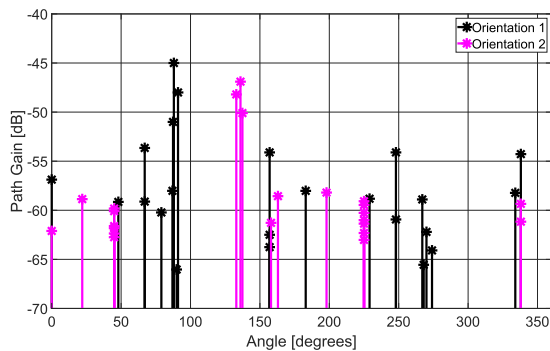
FIGURE 10. Estimated DoA of self-generated signal using SAGE.

orientation 1 and 135° for orientation 2. The remaining paths have much lower power and are assumed as noise.

Results presented in this section validate the correct performance of the proposed testbed, as both methods indicate the expected DoA. This preliminary measurement was an important step to show the proper operation of the proposed calibration system and assures that the post-processing methodology can be used with over-the-air transmitted signals. However in this test, only the self-generated LTE signal was used. Therefore, second measurement campaign was performed in which the live LTE signals were recorded.

B. MEASUREMENTS USING LIVE LTE NETWORK

After measurements using self-generated LTE signal, the target of the second campaign was to validate the performance of the measurement testbed and post-processing using live LTE signals, with inherited interference from other cells. The measurement equipment was put inside a university van and transported to rural location as shown on Figure 11.

In this location the same set of tests as explained in the previous section were performed. 100 ms snapshots were recorded twice. In between two recordings, the antenna array was turned by 180°. The array was again placed in the LoS conditions with respect to the base station located approximately 1.5 km away. Based on GPS coordinates of the van and the serving Base Station, it was determined that the expected angles are approximately 230° for the first orientation of the array and 50° in its second position. During the post-processing, the decoded serving Cell ID was carefully checked to belong to the expected Base Station.

Figures 12 and 13 present the obtained results using beam sweep and SAGE respectively. Using both methods and for two considered orientations of the array the maximum SINR and path gain correspond to the expected angle. It is worth to notice that the computed SINR is much higher than in the first test using self-generated signal. Even though the distance from the receiver to the base station was much longer with respect to the first tests, the considerable increase of transmit power (real base stations transmit with power above 40 dBm while our transmitter was set only to 0 dBm) contributes to the increased SINR values. Contrary to the self-generated signal, as shown on Figure 12, the SINR difference between its peak
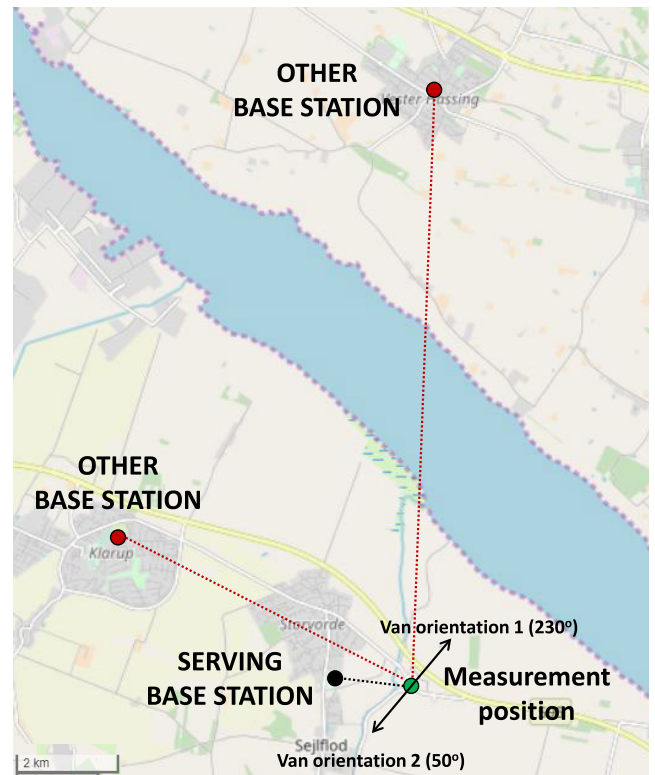
FIGURE 11. Location of the measurement campaign with real LTE signals.
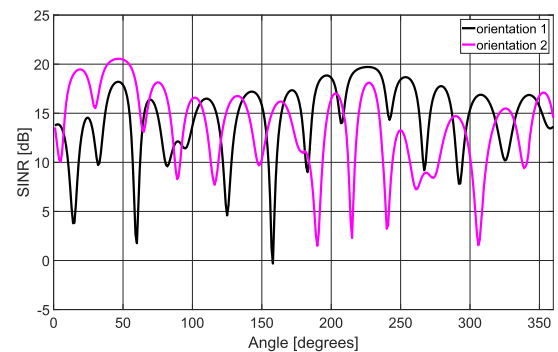
FIGURE 12. Angular distribution of SINR for real LTE signal.

values at the expected DoAs and the values for other angles is much lower than in case of the self-generated signal. It is an expected behavior as even in a LoS scenario, due to distance between the transmitter and the receiver the level of multipath is higher than in the first experiment where a low power self-generated signal was transmitted only from 50 m distance.

Results obtained in this section show, that the proposed testbed and post-processing methodology can reliably be used for various research activities. First, they validate the correct reception and demodulation of real LTE signals, a fundamental step required before any further research activity can be conducted. The correct DoA estimation shows the robustness of the setup even in the presence of interfering signals coming from different cells further expanding the potential of the proposed testbed.
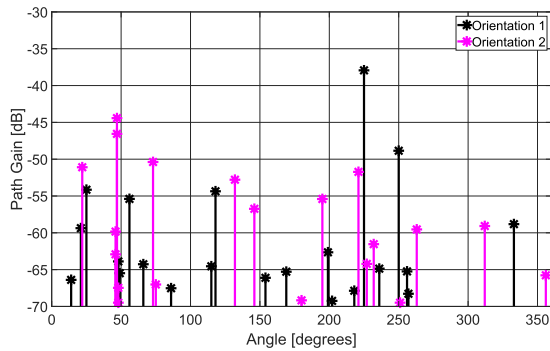
FIGURE 13. Estimated DoA of real LTE signal using SAGE.

VII. POTENTIAL APPLICATIONS OF THE MEASUREMENT TESTBED

In this Section a set of possible options for testbed usage is discussed. Some of the applications are related to the already conducted research activities, while others are planned as a future work or are foreseen as new potential projects. The objective of this section is to give the reader a perspective on how the testbed can be used and to encourage a reflection on its other possible applications.

A. CONDUCTED MEASUREMENT CAMPAIGNS

At the time of writing this article, the proposed testbed was already used by the authors in two different measurement campaigns. In the first campaign, related to studies of Vehicle-to-Network (V2N) communications, described testbed was placed inside a car with the antenna array installed on its roof and multiple drive tests were performed in which more than 6000 snapshots were recorded in different environments. The recorded data was used for different research purposes.

First, for validating the performance of multi-antenna receivers: beamforming and MRC are studied in [29]. The study focuses on the downlink interference observed by a vehicle and its impact on beamforming and MRC performance. It is observed that, on average, the performance of both receivers is comparable. However in the situations where there is one single dominant interferer coming from a specific direction, the use of receive beamforming can help mitigating this interference by steering the beam in the different direction and leads to average 3 dB SINR improvement over the MRC receiver that performs diversity combining. Moreover, in post-processing by taking the signal from only one antenna stream and removing the remaining ones, the single antenna receiver is emulated and used in comparison with multi-antenna receivers to showcase the expected antenna processing gains.

The same dataset was processed using SAGE in [30]. The focus of this work is on experimental assessment of uplink beamforming on the vehicle terminal. In the first part, three different direction acquisition methodologies: beam sweeping, DoA estimation and naive beamforming towards the direct path to the serving cell are compared to understand the

FIGURE 14. Designed testbed lifted in the air during measurement campaign focusing on a UAV A2G channel characterization.

trade-off between their complexity and accuracy. It was determined that the beamforming direction obtained using beam sweeping methodology tends to lead to higher overall SINR than by using DoA estimation. Not surprisingly, in clear LoS scenarios, the DoA estimation leads to comparable SINR as naive beamforming towards the direct path to the serving cell.

In the second part of this study, after DoA estimation of each snapshot using SAGE, two different direction tracking algorithms are studied to understand their possible use to alleviate the frequency of time-consuming direction acquisition. By comparing the estimated DoA using SAGE with the prediction of the tracking algorithm, it was determined that in rural and suburban scenarios, the directions of incoming signals can be predicted without the need for performing any direction acquisition even for distances exceeding 1 km. Finally, the impact of 3-dB beamwidth of the antenna beam on the tracking algorithm's performance is studied.

Second measurement campaign conducted using the proposed setup was targeted to better understand propagation characteristics of the Air-to-Ground (A2G) channel between a cellular-connected UAV and a base station. As can be seen on Figure 14, the proposed setup was placed inside a cage and lifted with a crane in order to record cellular signals in the air up to 40 m.

The work in [31] is related to spatial channel characterization of the A2G channel and targets the changes in the main

path's DoA during the vertical flight of a UAV. Snapshots recorded at a different heights are used as an input for SAGE to estimate DoAs of incoming signals. Moreover, by computing the Angular Spread (AS) of the incoming signals for different heights and measured environments, the authors study from which height one can assume that only the dominant LoS path between a Base Station and a UAV exists and the impact of multipath components can be neglected. Surprisingly the results show that even 20 m above the roofs of the buildings, the multipath components still contribute to the overall received signal power and cannot be neglected.

Finally in [28], similar to the previously described application, the very same snapshots recorded in the air were used to compare the performance of multi-antenna receivers in UAV scenarios. In contrast to the results obtained during the vehicular campaign, in the air the beamforming constantly outperforms MRC receiver. It is related to the fact that, comparing with ground, more often there is a dominant strong LoS path from the transmitter. When beamformed towards this direction, the MRC receiver can be outperformed.

B. FUTURE WORK AND OTHER TESTBED APPLICATIONS
In the future work, the same recorded data snapshots can be further post-processed. So far only the conventional beamforming, pointing towards the estimated DoA was studied. Different beamforming algorithms as for example null-steering or side lobe level reduction techniques can be implemented to study their potential to mitigate the strongest interferers and therefore further improve the received SINR. Up to this point, the performed channel characterization for the A2G channel focused only on the spatial properties of the incoming signals. Contrary to the work in [27] other parameters including Path Loss or delay spread were not yet examined and can be a part of a future work.

The proposed testbed and the described measurement activities are expected to be easily adjustable when the new 5th Generation (5G) networks becomes widely available. As already described in the introduction, 5G with its new use cases will open the possibility for more studies on various channel and system-level functionalities. It is presumed that the proposed general design would remain valid and only the implementation specific parameters such as operating frequency (and therefore antenna array) or recorded bandwidth would have to be adjusted. In order to cope with large 5G bandwidths (up to 100 MHz), it may be necessary to replace the currently-used USRP boards with a model allowing to record larger bandwidths. In case the proposed post-processing method, based on the LTE toolbox, the complimentary 5G toolbox is already available and could potentially be used as a replacement.

Although the presented testbed was designed to receive the LTE signals (both self-generated and live from deployed customer networks), it may also be used to receive any kind of excitation signal provided the operating frequency and bandwidth are within the limits of the USRP boards and that the used antennas are suitable to receive signals from the

target frequency band. This paves the way for a new variety of use cases. One example can be the experimental validation of channel charting algorithms [32]. The main concept of channel charting can be summarized as an user localization technique performed by the network, based only on the received estimated UL channel. If the signals are recorded with a multi-antenna system, the slowly changing features such as DoA can be estimated. Provided that many samples from different locations are recorded (and therefore multiple copies of estimated UL channel are obtained) several machine learning algorithms are used to map these slowly changing channel features into the precise estimation of user's position. By deploying an extra transmitter with a self-generated signal, the proposed multi-antenna testbed can be used to record these signals. Later in the post-processing the charting algorithms can be validated.

VIII. CONCLUSION
In this work a large multi-antenna measurement setup used to record multi-site cellular signals such as LTE is presented. It can be used for various research activities including multi-antenna channel characterization in the emerging use cases such as V2X or UAV communications. After hardware description, a calibration method required for phase alignment of USRPs is proposed and validated during measurement campaigns with self-generated LTE signals. Two post-processing methods were discussed using Matlab LTE testbed for beamforming evaluation and SAGE for channel parameter estimation. Finally, results from measurement campaigns are discussed, where live LTE signals were recorded and used for DoA estimation using both SAGE and beam sweeping methodologies. The setup is shown to be a versatile tool, perfectly suitable to record signals incoming concurrently from multiple transmitters in situations where the same recorded raw I&Q samples can be used for many diverse research activities.

REFERENCES
[1] A. Goldsmith, S. A. Jafar, N. Jindal, and S. Vishwanath, "Capacity limits of MIMO channels," *IEEE J. Sel. Areas Commun.*, vol. 21, no. 5, pp. 684–702, Jun. 2003.

[2] W. Wang, S. L. Capitaneanu, D. Marinca, and E.-S. Lohan, "Comparative analysis of channel models for industrial IoT wireless communication," *IEEE Access*, vol. 7, pp. 91627–91640, 2019.

[3] M. Yang, B. Ai, R. He, L. Chen, X. Li, J. Li, B. Zhang, C. Huang, and Z. Zhong, "A cluster-based three-dimensional channel model for vehicle-to-vehicle communications," *IEEE Trans. Veh. Technol.*, vol. 68, no. 6, pp. 5208–5220, Jun. 2019.

[4] B. Van Der Bergh, A. Chiumento, and S. Pollin, "LTE in the sky: Trading off propagation benefits with interference costs for aerial nodes," *IEEE Commun. Mag.*, vol. 54, no. 5, pp. 44–50, May 2016.

[5] *WINNER II Channel Models*, document IST-4-027756 WINNER II D1.1.2 V1.2, Sep. 2007.

[6] D. A. Wassie, I. Rodriguez, G. Berardinelli, F. M. L. Tavares, T. B. Sørensen, T. L. Hansen, and P. Mogensen, "An agile multi-node multi-antenna wireless channel sounding system," *IEEE Access*, vol. 7, pp. 17503–17516, 2019.

[7] G. G. Joshi, C. B. Dietrich, Jr., and W. L. Stutzman, "Adaptive beamforming measurements using four-element portable and mobile arrays," *IEEE Trans. Antennas Propag.*, vol. 53, no. 12, pp. 4065–4072, Dec. 2005.

[8] (2017). *Matlab LTE System Toolbox Reference Page*. [Online]. Available: https://ch.mathworks.com/products/lte-system.html

[9] B. H. Fleury, D. Dahlhaus, R. Heddergott, and M. Tschudin, "Wideband angle of arrival estimation using the SAGE algorithm," in *Proc. IEEE Int. Symp. Spread Spectr. Techn. Appl. (ISSSTA)*, vol. 1, Sep. 1996, pp. 79–85.

[10] C. M. Simmonds and M. A. Beach, "Downlink calibration requirements for the TSUNAMI (II) adaptive antenna testbed," in *Proc. 9th IEEE Int. Symp. Pers., Indoor Mobile Radio Commun.*, vol. 3, Sep. 1998, pp. 1260–1264.

[11] R. Wang, C. U. Bas, O. Renaudin, S. Sangodoyin, U. T. Virk, and A. F. Molisch, "A real-time MIMO channel sounder for vehicle-to-vehicle propagation channel at 5.9 GHz," in *Proc. IEEE Int. Conf. Commun. (ICC)*, May 2017, pp. 1–6.

[12] C. Scarborough, K. Venugopal, A. Alkhateeb, and R. W. Heath, Jr., "Beamforming in millimeter wave systems: Prototyping and measurement results," in *Proc. IEEE 88th Veh. Technol. Conf. (VTC-Fall)*, Aug. 2018, pp. 1–5.

[13] R. M. Rao, W. Zhu, S. Lang, C. Oberli, D. Browne, J. Bhatia, J.-F. Frigon, J. Wang, P. Gupta, H. Lee, D. N. Liu, S. G. Wong, M. Fitz, B. Daneshrad, and O. Takeshita, "Multi-antenna testbeds for research and education in wireless communications," *IEEE Commun. Mag.*, vol. 42, no. 12, pp. 72–81, Dec. 2004.

[14] Y. Amano, T. Inoue, and H. Shinonaga, "Performances of beamforming in downlink with smart antenna testbed," in *Proc. IEEE 56th Veh. Technol. Conf.*, vol. 1, Sep. 2002, pp. 77–81.

[15] K. Nishimori, R. Kudo, N. Honma, Y. Takatori, O. Atsushi, and K. Okada, "Experimental evaluation using 16 × 16 multiuser MIMO testbed in an actual indoor scenario," in *Proc. IEEE Antennas Propag. Soc. Int. Symp.*, Jul. 2008, pp. 1–4.

[16] Ó. Gonzalez, D. Ramírez, I. Santamaria, J. A. García-Naya, and L. Castedo, "Experimental validation of interference alignment techniques using a multiuser MIMO testbed," in *Proc. Int. ITG Workshop Smart Antennas*, Feb. 2011, pp. 1–8.

[17] R. Weinmann, M. Tangemann, S. Fritsch, and C. Hoek, "Beamforming performance measurements in a DCS 1800 smart antenna testbed," in *Proc. 48th IEEE Veh. Technol. Conf. Pathway Global Wireless Revolution*, vol. 2, May 1998, pp. 1024–1028.

[18] J. M. V. Burgos, E. Gago-Cerezal, V. A. Gracia, and L. M. C. Cervera, "DEMIURGO, an SDR testbed for distributed MIMO," in *Proc. 3rd Int. Symp. Wireless Commun. Syst.*, Sep. 2006, pp. 210–213.

[19] W. Xiong, J. Lu, X. Tian, G. Chen, K. Pham, and E. Blasch, "Cognitive radio testbed for digital beamforming of satellite communication," in *Proc. Cognit. Commun. Aerosp. Appl. Workshop (CCAA)*, Jun. 2017, pp. 1–5.

[20] J. Vieira, S. Malkowsky, K. Nieman, Z. Miers, N. Kundargi, L. Liu, I. Wong, V. Öwall, O. Edfors, and F. Tufvesson, "A flexible 100-antenna testbed for massive MIMO," in *Proc. IEEE Globecom Workshops (GC Wkshps)*, Dec. 2014, pp. 287–293.

[21] P. Harris, W. B. Hasan, S. Malkowsky, J. Vieira, S. Zhang, M. Beach, L. Liu, E. Mellios, A. Nix, S. Armour, A. Doufexi, K. Nieman, and N. Kundargi, "Serving 22 users in real-time with a 128-antenna massive MIMO Testbed," in *Proc. IEEE Int. Workshop Signal Process. Syst. (SiPS)*, Oct. 2016, pp. 266–272.

[22] D. Gaydos, P. Nayeri, and R. Haupt, "Experimental demonstration of a software-defined-radio adaptive beamformer," in *Proc. 48th Eur. Microw. Conf. (EuMC)*, Sep. 2018, pp. 1581–1584.

[23] P. Nayeri and R. L. Haupt, "A testbed for adaptive beamforming with software defined radio arrays," in *Proc. IEEE/ACES Int. Conf. Wireless Inf. Technol. Syst. (ICWITS) Appl. Comput. Electromagn. (ACES)*, Mar. 2016, pp. 1–2.

[24] N. Tayem, M. Omer, and A. A. Hussain, "Hardware implementation of MUSIC and ESPRIT on NI-PXI platform," in *Proc. IEEE Mil. Commun. Conf.*, Oct. 2014, pp. 329–332.

[25] B. Rares, C. Codau, A. Pastrav, T. Palade, H. Hedesiu, B. Balauta, and E. Puschita, "Experimental evaluation of AoA algorithms using NI USRP software defined radios," in *Proc. 17th RoEduNet Conf., Netw. Edu. Res. (RoEduNet)*, Cluj-Napoca, Romania, Sep. 2018, pp. 1–6.

[26] M. Willerton, D. Yates, V. Goverdovsky, and C. Papavassiliou, "Experimental characterization of a large aperture array localization technique using an SDR testbench," in *Proc. Wireless Innov. Forum Conf. Commun. Technol. Softw. Defined Radio (SDR)*, Dec. 2011, pp. 1–7.

[27] X. Cai and J. Rodríguez-Piñeiro, X. Yin, N. Wang, B. Ai, G. F. Pedersen, and A. P. Yuste, "An empirical air-to-ground channel model based on passive measurements in LTE," *IEEE Trans. Veh. Technol.*, vol. 68, no. 2, pp. 1140–1154, Feb. 2019.

[28] T. Izydorczyk, M. Bucur, F. M. L. Tavares, G. Berardinelli, and P. Mogensen, "Experimental evaluation of multi-antenna receivers for UAV Communication in Live LTE networks," in *Proc. IEEE Globecom Workshops (GC Wkshps)*, Dec. 2018, pp. 1–6.

[29] T. Izydorczyk, F. M. L. Tavares, G. Berardinelli, M. Bucur, and P. Mogensen, "Performance evaluation of multi-antenna receivers for vehicular communications in live LTE networks," in *Proc. IEEE 89th Veh. Technol. Conf. (VTC-Spring)*, Apr./May 2019, pp. 1–6.

[30] T. Izydorczyk, G. Berardinelli, F. M. L. Tavares, M. Bucur, and P. Mogensen, "On the potential of uplink beamforming in vehicular networks based on experimental measurements," in *Proc. IEEE 90th Veh. Technol. Conf. (VTC-Fall)*, Sep. 2019, pp. 1–5.

[31] T. Izydorczyk, F. M. L. Tavares, G. Berardinelli, M. Bucur, and P. Mogensen, "Angular distribution of cellular signals for UAVs in urban and rural scenarios," in *Proc. 13th Eur. Conf. Antennas Propag. (EuCAP)*, Mar. 2019, pp. 1–5.

[32] C. Studer, S. Medjkouh, and E. Gönültaş, T. Goldstein, and O. Tirkkonen, "Channel charting: Locating users within the radio environment using channel state information," *IEEE Access*, vol. 6, pp. 47682–47698, 2018.

TOMASZ IZYDORCZYK received the M.Sc. degree in mobile communications from Telecom ParisTech/Eurecom, in 2017. He is currently pursuing the Ph.D. degree with Aalborg University (AAU). In 2016, he was a Research Intern with Intel Mobile Communications, Sophia Antipolis, France. His research interests include MIMO techniques for V2X and UAV communications, focusing on their experimental verification.

FERNANDO M. L. TAVARES received the M.Sc. degree from the University of Brasilia, Brazil, in 2009, and the Ph.D. degree from Aalborg University, Denmark, in 2015, in wireless communications. He has been a Visiting Researcher with Nokia Bell Labs Denmark, since 2011. He is currently an Assistant Professor in wireless communication networks with Aalborg University. His research interests include MIMO, interference management, and advanced transceiver design.

GILBERTO BERARDINELLI received the first and second level degrees (*cum laude*) in telecommunication engineering from the University of L'Aquila, Italy, in 2003 and 2005, respectively, and the Ph.D. degree from Aalborg University, Denmark, in 2010. He is currently an Associate Professor with the Wireless Communication Networks (WCN) Section, Aalborg University, and also working in tight cooperation with Nokia Bell Labs. His research interests include mostly focused on physical layer, medium access control, and radio resource management design for 5G systems. He is the author or coauthor of more than 100 international publications, including conference proceedings, journal contributions, and book chapters.

PREBEN MOGENSEN received the M.Sc. and Ph.D. degrees from Aalborg University, in 1988 and 1996, respectively. Since 1995, he has been a part-time associated with Nokia. Since 2000, he has also been a Full Professor with Aalborg University, where he is currently leading the Wireless Communication Networks Section. He is also a Principal Scientist with Nokia Bell Labs and a Nokia Bell Labs Fellow. He has coauthored over 400 articles in various domains of wireless communication. His Google Scholar H-index is 61. His current research interest includes the 5G industrial IoT and technology components towards 6G.

● ● ●